Asian Journal of Andrology (2017) 19, 659–665
www.asiaandro.com; www.ajandrology.com

Open Access

ORIGINAL ARTICLE

Sperm Biology

Characterization of MAGEG2 with testis-specific expression in mice

Juri Jeong, Sora Jin, Heejin Choi, Jun Tae Kwon, Jihye Kim, Jaehwan Kim, Zee Yong Park, Chunghee Cho

Male germ cell development is a well-defined process occurring in numerous seminiferous tubules of the testis. Uncovering testicular novel genes related to intrinsic regulation of spermatogenesis is essential for the understanding of spermatogenesis. In the present study, we investigated mouse *Mageg2*, which belongs to a group of melanoma-associated antigens (MAGEs). *Mageg2* is transcribed in the testis specifically, and its expression level is increased at the pachytene spermatocyte stage, indicating that *Mageg2* is expressed predominantly in germ cells. We generated an antibody against mouse MAGEG2 for further characterization at the protein level. Immunoblot analysis suggested that MAGEG2 has specific testicular expression and the expression primarily occurred in pachytene spermatocytes. Proteomic analyses demonstrated that mouse MAGEG2 binded to testicular germ cell-specific serine/threonine-protein kinase 31 (STK31) and heat shock protein 9 (HSPA9). Direct binding with both interaction partners was confirmed by co-immunoprecipitation. We found that STK31 and HSPA9 bind MAGEG2 directly but not with each other. Interestingly, MAGEG2 reduced the kinase activity of STK31. Our study suggests that mouse MAGEG2 has at least two functions, including chaperone activity related to HSPA9 and regulation of pachytene spermatocyte-specific kinase, STK31. Altogether, our results provide the first information about MAGEG2 at the transcript and protein levels and suggest its potential molecular functions.
Asian Journal of Andrology (2017) **19**, 659–665; doi: 10.4103/1008-682X.192033; published online: 15 November 2016

Keywords: heat shock proteins; serine/threonine kinase; spermatogenesis; testis

INTRODUCTION

Spermatogenesis is a pivotal process in most mammals because successful male germ cell development is associated with the maintenance and generation of organisms. This process occurs in seminiferous tubules containing developing germ cells in numerous concentric layers and somatic cells, the Sertoli cells.[1] Germ cells proliferate by repeated mitotic proliferation, meiotic divisions, and morphological changes, which consist of DNA replication, genetic recombination, reduction of chromosomes, and morphological changes to produce haploid spermatids.[2] Thus, to achieve successful spermatogenesis, highly ordered regulations and well-conditioned program of gene expression are required.

Gene expression for male germ cell development occurs at three levels: intrinsic, interactive, and extrinsic.[3] As a highly conserved genetic program, the intrinsic program determines which genes are utilized and when they are expressed in germ cells for their proliferation. The interactive process represents associations between germ cells and somatic cells in the seminiferous tubules. The interactive program depends on the extrinsic program, which reflects hormonal regulation of the somatic cells by testosterone and follicle-stimulating hormone.[3,4] These regulatory processes provide a comprehensive network of genes controlling male reproduction. In particular, the intrinsic program operates gene expression patterns for germ cell progression in a time-dependent manner. Therefore, identification of testis-specific genes and elucidation of developmental stage-specific mechanisms related to the intrinsic genetic program are valuable for understanding male reproduction.

In this study, we performed *in silico* screening using the Sertoli cell UniGene library (http://www.ncbi.nlm.nih.gov/unigene) to search for testis-specific novel genes in mice. The normalization process of expressed sequence tag (EST) information was performed by the concept of transcript per million (TPM).[5] With the calculated testis specificity, mouse *Mageg2* was selected since it was found only in the Sertoli cell library and not in other testis-related libraries. Because the mouse *Mageg2* contains a conserved domain of the melanoma-associated antigen (MAGE) family and is located on mouse chromosome 19, it was classified as a Type II MAGE, but very little information is available so far.

The MAGE family is well characterized as a subgroup of cancer/testis antigens (CT antigens)[6] containing conserved ~170 amino acid residues, the MAGE homology domain (MHD).[7,8] CT antigens are a category of protein antigens with restricted expression in developing germ cells in the testis and malignant tumors but not in other normal somatic tissues.[9] The MAGE family is categorized into two subfamilies, I and II, on the basis of their chromosomal location and expression.[10,11] The Type I MAGEs, including MAGE-A, -B, and -C, are CT antigens and are clustered on the X chromosome. In contrast, the other MAGEs, which are not restricted to the X chromosome, are classified as Type II MAGEs.[12] The Type II MAGEs are ubiquitously expressed in various normal tissues and have functions in cell cycle arrest, neuronal differentiation, and apoptosis.[12,13]

School of Life Sciences, Gwangju Institute of Science and Technology, Gwangju 61005, South Korea.
Correspondence: Dr. C Cho (choch@gist.ac.kr)
Received: 28 July 2016; Revised: 12 September 2016; Accepted: 08 October 2016

No functional study of MAGE proteins related to spermatogenesis has been reported yet in mice. Here, we identified a novel MAGE Type II family member, MAGEG2, which is a testis-specific protein primarily expressed in pachytene spermatocytes and whose expression is regulated in a stage-specific manner. Proteomic examination identified serine/threonine-protein kinase 31 (STK31) and heat shock protein 9 (HSPA9) as binding partners of MAGEG2. We found that MAGEG2 is repressive to one of the major interaction partners, STK31. Our study suggests that MAGEG2 has various cellular activities during spermatogenesis.

MATERIALS AND METHODS

Cell culture and transient transfection

Mouse fibroblast cell line (NIH3T3, CRL-1658) and human embryonic kidney cell line (HEK293T, CRL-11268) cells were obtained from the American Type Culture Collection (ATCC, Manassas, VA, USA). Cells were grown in Dulbecco's Modified Eagle's medium (DMEM, Invitrogen, Carlsbad, CA, USA) supplemented with 10% (*v/v*) fetal bovine serum (FBS, Gibco BRL, Grand Island, NY, USA) and 1% (*v/v*) penicillin/streptomycin (Gibco BRL) at 37°C in an atmosphere of 5% (*v/v*) CO_2. Cell culture media were changed every 1–2 days and cells were subcultured every 3–4 days. For transfection into the NIH3T3 cell line, full-length cDNA of *Mageg2* was inserted into pEGFP-N2 vector (Clontech, Mountainview, CA, USA). For transfection into the HEK293T cells, full-length DNA construct of *Mageg2* was cloned into pcDNA™ 3.1/myc-His B vector (Invitrogen) and HA-STK31 was generated by transfection into pHM6 vector (Roche, Basel, Switzerland). All transient expressions of cloned vectors were achieved using Lipofectamine™ LTX (Invitrogen) transfection reagent, according to the manufacturer's protocol. Empty vectors were used as controls for inserted vectors. In the case of expression of GFP-tagged MAGEG2, at 48 h after transfection, cells were fixed with 4% (*v/v*) paraformaldehyde, stained with Hoechst 33258 (Sigma-Aldrich, St. Louis, MO, USA), and mounted on a glass slide. In the case of introduction of Myc-tagged MAGEG2 or HA-tagged STK31, transfected cells were collected after 24 h with 1% (*v/v*) Nonidet P-40 (NP-40) lysis buffer for subsequent experiments.

Total RNA extraction and reverse transcription-polymerase chain reaction (RT-PCR)

Total RNA was isolated with the TRI Reagent® (Molecular Research Center, Cincinnati, OH, USA) following the manufacturer's instructions, from different tissues (liver, spleen, kidney, lung, skeletal muscle, brain, heart, and testis) of 8-week-old ICR male mice. To examine the developmental expression patterns in the testis, total RNAs were obtained from different stages of male mice (aged 8, 10, 12, 14, 16, 20, 30, and 84 days), as well as from germ cell-deficient testes of W/W^v mice for investigation of germ cell-specific expression. Then, for elimination of genomic DNA contamination, 2 U of DNase I (New England Biolabs, Ipswich, MA, USA) was treated at 37°C for 30 min and inactivated by addition of 5 mmol l^{-1} EDTA. Complementary DNAs (cDNAs) were synthesized by random primer and oligo (dT) primer using Omniscript reverse transcriptase (Qiagen, Hilden, Germany). RT-PCR was conducted using a specific primer set for the *Mageg2* transcript (forward, 5′-ACCAGAGAACGCCCACCACCG-3′, and reverse, 5′-CCCTACGCTGCTCATCCGCCA-3′). The cDNA levels were calibrated by amplification of glyceraldehyde-3-phosphate dehydrogenase (Gapdh) (forward, 5′-AGCCAAAAGGGTCATCTCCG-3′, and reverse, 5′-TCCTCAGTGTAACCCAAGATGCC-3′). Amplification was carried out with the following conditions: initial treatment for 5 min at 94°C, followed by 30 cycles of 94°C for 30 s, 60°C for 30 s, and 72°C for 30 s. All animal investigations were carried out according to the guidelines of the Animal Care and Use of Gwangju Institute of Science and Technology (Permit number: GIST2014-171).

Antibodies

To generate a polyclonal antibody against mouse MAGEG2, synthesized antigen peptides were immunized into male New Zealand white rabbits aged 4–6 months (body weight 2.5 kg). Glutathione S-transferase (GST) fusion protein was designed as an antigen peptide, with the PCR product corresponding to residues 156–294 of MAGEG2 constructed in pGEX-5X-2 (GE Healthcare, Little Chalfont, UK). The recombinant vector was confirmed by sequencing, and then the vector was transformed into *Escherichia coli* BL21 (DE3). GST fusion MAGEG2 proteins were induced by addition of 0.1 mmol l^{-1} isopropyl-β-D-thiogalactopyranoside (IPTG, Sigma-Aldrich, St. Louis, MO, USA) and subsequently purified with glutathione Sepharose 4B (GE Healthcare, Little Chalfont, UK). Isolated GST-MAGEG2 fusion proteins were injected for generation of polyclonal antibodies by Macrogen (Seoul, Korea). The antibodies were affinity purified with corresponding antigens using AminoLink Immobilization kit (Pierce, Waltham, MA, USA). Monoclonal anti-α-tubulin antibody (05-829) and monoclonal anti-ADAM2 antibody (MAB19292) were purchased from Millipore (Billerica, MA, USA). Polyclonal anti-GAPDH antibody was obtained from AbFrontier (LF-PA0212, Seoul, Korea). Monoclonal anti-Myc antibody for Western blot analysis was purchased from Cell Signaling (#2276, Danvers, MA, USA) and monoclonal anti-Myc antibody for immunoprecipitation was obtained from Santa Cruz Biotechnology (SC-40, Santa Cruz, CA, USA). Polyclonal anti-HA antibody was purchased from Abcam (Ab9110, Cambridge, UK). Horseradish peroxidase (HRP)-conjugated anti-rabbit IgG and anti-mouse IgG (Jackson ImmunoResearch, West Grove, PA, USA) were used as secondary antibodies.

Preparation of protein samples and Western blot analysis

Whole cell lysates were extracted with 1% NP-40 lysis buffer containing protease inhibitor cocktail on ice by homogenization. The homogenates were incubated on ice for 30 min, and cell debris was pelleted by centrifugation at 19 326 *g*, 4°C for 10 min. Proteins of the supernatant were obtained and their concentration measured with the BCA assay (Thermo, Waltham, MA, USA). Then, lysate samples were suspended in 2 × SDS sample buffer containing 5% (v/v) β-mercaptoethanol, boiled for 10 min, and centrifuged at 19 326 *g*, 4°C for 10 min. The protein samples were loaded into SDS-polyacrylamide gel electrophoresis (PAGE) and transferred onto polyvinylidene fluoride (PVDF) membrane (Pall Corporation, East Hills, NY, USA). Membranes were blocked in TBS-T containing 5% (*v/v*) nonfat dry milk (BD Biosciences, San Jose, CA, USA) for 1 h at room temperature, and the blots were incubated overnight at 4°C with primary antibodies. After being washed three times with TBS-T, the membranes were incubated with secondary antibodies for 1 h at room temperature. Following three washes, the blots were developed with electrogenerated chemiluminescence (ECL, Pierce).

Preparation of testicular cells, testicular spermatozoa, and mature spermatozoa

Cells were isolated from 8-week-old ICR male mice in Mg^{2+}-Hepes buffer. Testicular germ cells and testicular spermatozoa were separated by 52% (*v/v*) gradient of isotonic Percoll (GE Healthcare) and centrifuged for 10 min (27 000 *g*, 4°C), and the isolated cells were resuspended with Mg^{2+}-Hepes buffer.[14] Mature spermatozoa were prepared from the cauda epididymidis and vas deferens with PBS buffer. After being washed with PBS buffer, the collected cells were directly boiled in 1 × SDS sample buffer containing 5% (*v/v*) β-mercaptoethanol.

Immunoprecipitation

Testes and cells were lysed with 1% (*v/v*) NP-40 lysis buffer, and 1 mg of lysates was incubated overnight at 4°C with the recommended amount of antibodies under rotary agitation (5 μg anti-MAGEG2; 4 μg anti-Myc; 4 μg anti-HA; 2 μg anti-HSPA9). For IP-kinase assay, 0.5 mg of cell lysates was incubated with 3 μg of anti-STK31 antibodies and protein A sepharose beads (GE Healthcare) were added and incubated for an additional 6 h at 4°C with shaking. The binding was stopped by washing three times with lysis buffer, and then the immunocomplexes were boiled in 1 × SDS sample buffer containing 5% (*v/v*) β-mercaptoethanol for further western blot analysis or resuspended in kinase buffer for subsequent kinase assay. The immunoprecipitated proteins were eluted by 8 mol l^{-1} urea for subsequent proteomic analysis and capillary reversed-phase liquid chromatography-tandem mass spectrometry as described previously.[15]

Immunoprecipitation (IP)-kinase assay

For kinase reaction, STK31 was prepared by immunoprecipitation on protein A sepharose beads (GE Healthcare) with anti-STK31 using transfected cell extracts of single transfection with HA-STK31 and double transfection with both HA-STK31 and Myc-MAGEG2. The efficiency of immunoprecipitation was evaluated by western blot analysis on one-quarter of both proteins. One-half of the immunoprecipitated beads were suspended in kinase reaction buffer supplemented with 32 μg of myelin basic protein (MBP, Enzo Life Sciences, Farmingdale, NY, USA) as a substrate and the reactions were initiated by addition of 0.2 m mol l^{-1} ATP/Mg^{2+} (Sigma-Aldrich) containing 10 μCi of (γ-^{32}P) ATP (3000 Ci·mmol l^{-1}, Perkin-Elmer, Waltham, MA, USA). The mixture was incubated for 1 h at 30°C for kinase reaction and the reaction was stopped by boiling in SDS sample buffer containing 5% (*v/v*) β-mercaptoethanol. The kinase reaction was visualized by autoradiography of SDS PAGE gel.

RESULTS

Phylogenetic relationship of MAGEG2

As a first step toward characterization of mouse MAGEG2, we studied the phylogenetic relationship by examining gene information from NCBI databases (**Figure 1**). The mouse *Mageg2* gene is composed of a single exon that encodes 294 amino acid residues predicted as a 33 kDa protein. The mouse MAGEG2 protein contains MHD in its middle region (residues 82–253) and it has 65% and 67% identities with human and mouse necdin-like protein 2 (NDNL2, MAGEG1), respectively. The EST profile in the UniGene database of *Mageg2* was restricted to the testis in contrast to those of other Type II MAGEs.

Mageg2 expression patterns at the transcript and protein levels

On the basis of the information from *in silico* analysis, expression profiles of transcript and protein level were examined. First, a transcriptional study was carried out. To determine whether *Mageg2* is an authentic testis-specific gene, tissue distribution was investigated by RT-PCR with cDNAs from different mouse tissues: liver, spleen, kidney, lung, skeletal muscle, brain, heart, and testis (**Figure 2a**), in which *Mageg2* showed a testis-specific expression pattern. To determine which cells transcribe *Mageg2* in the testis, we carried out RT-PCR on germ cell-deficient mice (*W/W*^{v} mutant mice) (**Figure 2b**). The transcript

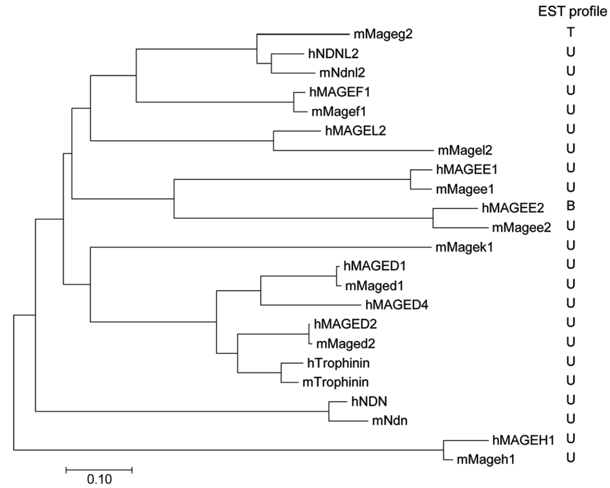

Figure 1: Phylogeny and subcellular localization of the mouse *Mageg2*. Phylogenetic tree of mouse and human type II MAGE family members. GeneBank accession numbers for the amino acid sequences used for phylogeny generation were NP_076270 (mouse *Mageg2*), NP_071432 (human *MAGEF1*), NP_619649 (human *NDNL2*), NP_075728 (mouse *Ndnl2*), NP_035012 (mouse *Ndn*), NP_002478 (human *NDN*), NP_061939 (human *MAGEL2*), NP_038807 (mouse *Magel2*), NP_109625 (mouse *Maged2*), NP_055414 (human *MAGED2*), NP_110428 (human *MAGED4*), NP_001005333 (human *MAGED1*), NP_062765 (mouse *Maged1*), NP_001002272 (mouse Trophinin), NP_001034794 (human Trophinin), NP_444431 (mouse *Magee1*), NP_065983 (human *MAGEE1*), NP_444436 (mouse *Magee2*), NP_619648 (human *MAGEE2*), NP_076277 (mouse *Mageh1*), NP_054780 (human *MAGEH1*). The phylogenetic tree was created by alignments with MUSCLE (multiple sequence comparison by log-expectation) and neighbor-joining tree was generated by MEGA7 software (molecular evolutionary genetics analysis). The tree was drawn to scale, with branch lengths in the same units as those of the evolutionary distances used to infer the phylogenetic tree. The evolutionary distances were computed using the Poisson correction method[49] and are in the units of the number of amino acid substitutions per site. Expected tissue distributions were marked with abbreviation of corresponding tissues (U: ubiquitously expressed, B: brain, T: testis).

of *Mageg2* was detected not only in the wild-type testis but also in the *W/W*^{v} mutant testis, indicating that *Mageg2* exists in germ cells and Sertoli cells in the testis. However, the mutant testis showed decreased band intensity compared with the wild-type testis. Thus, the expression of *Mageg2* is attributable in large to germ cells rather than to Sertoli cells. To analyze the expression pattern during germ cell development, RT-PCR was performed with mouse testis cDNAs obtained at different days after birth (8–84 days) (**Figure 2c**). The expression of *Mageg2* started before postnatal day 8, and then the expression level increased as spermatogenesis proceeds, especially around 16 days corresponding to the pachytene stage. These results indicate that the mouse *Mageg2* is expressed predominantly in germ cells in the testis. To analyze the protein characteristics *in vitro*, we examined subcellular localization with GFP-tagged full-length *Mageg2* in NIH3T3 cell lines. GFP signal was found in both nucleus and cytoplasm (**Supplementary Figure 1**).

Subsequent characterization at the protein level was performed with the polyclonal antibody generated against GST-tagged fusion protein (residues 156–294). Authenticity of the antibody was confirmed by comparative and competitive immunoblotting analyses (**Supplementary Figure 2**). The results of western blot analysis were similar to those of RT-PCR. MAGEG2 appeared to be expressed in the testis specifically (**Figure 2d**). Moreover, the protein existed not only in germ cells but also in Sertoli cells to the testis in a small

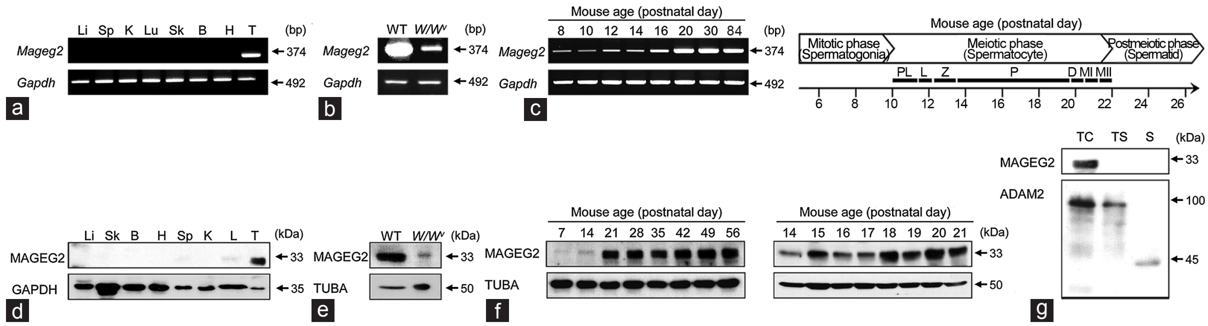

Figure 2: Expression patterns of *Mageg2* transcript and protein. To examine tissue distribution and expression patterns, RT-PCR and western blotting were carried out. (**a**) Tissue distribution of transcript level. cDNAs were obtained from adult mouse tissues. Li: liver; Sk: skeletal muscle; B: brain; H: heart; Sp: spleen; K: kidney; L: lung; T: testis. The glyceraldehydes-3-phosphate dehydrogenase (*Gapdh*) was used as a loading control. (**b**) Transcriptional estimation of the expression proportion in the testis by comparison of expression patterns between wild-type (WT) and germ cell-deleted (*W/W^v*) testis. (**c**) Developmental expression patterns at the transcript level. Stage-specific expression of *Mageg2* was examined in testes obtained from prepubertal and adult male mice (8, 10, 12, 14, 16, 20, 30, and 84 days). PL: preleptotene; L: leptotene; Z: zygotene; P: pachytene; D, diplotene; MI: meiotic division I; MII: meiotic division II. (**d**) Tissue distribution of protein level. Total cell lysates were prepared from different tissues of adult mice. An anti-GAPDH was used as a control. (**e**) MAGEG2 protein in WT and *W/W^v* testes. Total lysate from WT and germ cell-devoid testes of *W/W^v* mutant mice were blotted with the anti-MAGEG2 antibody. The antibody against α-tubulin was used as a loading control. (**f**) Stage-specific expression of MAGEG2 during spermatogenesis at the protein level. Immunoblotting was conducted with total lysates obtained from mouse testes on different days after birth. (**g**) Identification of cell type-specific expression during spermatogenesis. Total lysates from testicular germ cells (TC), testicular spermatozoa (TS), and mature spermatozoa (S) were utilized. Mouse ADAM2 (a disintegrin and metalloprotease 2), showing 100 kDa-precursor and 45 kDa-processed forms, was included as a protein control.

extent (**Figure 2e**). The developmental expression pattern from testes obtained at different times after birth was similar to that of the RNA level (**Figure 2f**). Especially during 14–21 postnatal days, the expression level increased steadily, suggesting that MAGEG2 is expressed majorly in pachytene spermatocytes. Expression of MAGEG2 in cells obtained from different cell stages during spermatogenesis was examined. MAGEG2 was expressed in testicular germ cells, not in testicular spermatozoa and mature spermatozoa, indicating developmentally regulated expression (**Figure 2g**).

Identification of putative binding partners of MAGEG2 by proteomic analysis

To investigate the functional characteristics of MAGEG2, it was necessary to determine the binding partners for MAGEG2. Thus, immunoprecipitation was carried out with whole cell lysate of the mouse testis, and then the precipitates were cleaved by tryptic digestion for liquid chromatography-MS/MS. The MS analysis detected seven proteins (**Table 1**), among which HSPA9 (mortalin) and STK31 were found at high spectrum counts. Although HSPA9 is well characterized as a member of the HSP70 family, there is little information related to spermatogenesis. STK31 has been identified as a germ cell-specific protein.[16,17] To certify as binding partners for MAGEG2, their characteristics at the protein level were examined. It was found that STK31 has testis specificity and HSPA9 was ubiquitously expressed (**Figure 3a**). Subsequently, comparison of expression patterns between normal and germ cell-lacking testes was performed (**Figure 3b**). STK31 was expressed in the *W/W^v* mutant testis at a lower level than in the normal testis (**Figure 3b**). Moreover, its expression in the testis was regulated developmentally (**Figure 3c** and **3d**), because abundance of expression occurred around day 14 when pachytene spermatocytes begin to appear and it showed limited expression in the testicular germ cells. On the contrary, as a ubiquitous protein, HSPA9 existed in both types of cells in the testis (**Figure 3b**) and it was expressed at all the developmental time points (**Figure 3c**). It primarily resided in mature spermatozoa (**Figure 3d**). These results collectively demonstrate that STK31 is developmentally regulated like MAGEG2. In the case of HSPA9, although overall expression patterns did not correspond to those of MAGEG2, the expression time of MAGEG2 overlapped with that of HSPA9.

Association of MAGEG2 with STK31 and HSPA9

To investigate the association of MAGEG2 with STK31 and HSPA9, we carried out *in vivo* immunoprecipitation analysis on mouse testis extract. **Figure 4a** shows that anti-MAGEG2 pulled down both STK31 and HSPA9 but not control IgG in normal rabbit serum. We also performed *in vitro* co-immunoprecipitation (co-IP). Myc-tagged MAGEG2 and HA-tagged STK31 were co-transfected into HEK293T cells, which do not contain either protein, but ubiquitous HSPA9 should be utilized as endogenous protein of the cell line. Efficiency of the transfection was verified by immunoblotting with anti-Myc and anti-HA (**Supplementary Figure 3**). STK31 and HSPA9 were co-immunoprecipitated with MAGEG2 similar to the result of *in vivo* analysis (**Figure 4b**), and conversely immunoprecipitation with anti-HA or anti-HSPA9 pulled down MAGEG2 (**Figure 4c** and **4d**). On the other hand, direct interaction between STK31 and HSPA9 was not observed through the co-IP (**Supplementary Figure 4**).

Repressive role of MAGEG2 for STK31

As a member of serine/threonine kinase, kinase activity of STK31 has been reported;[16] hence, we examined whether MAGEG2 regulates kinase activity of STK31. HEK293T cells were transfected only with HA-STK31 or subjected to co-transfection with Myc-MAGEG2 and HA-STK31. The efficiency of the co-transfection was examined by immunoblotting (**Figure 5a**). The confirmed cell lysate was immunoprecipitated with anti-STK31, and then the presence of both STK31 and MAGEG2 was determined by western blot analysis (**Figure 5b**). It was apparent that immunoprecipitated beads of the single transfection contained STK31 and the immunocomplex of double transfection was composed of both inserted proteins. Furthermore, STK31 in the immunoprecipitated beads with cognate antibody was utilized as kinase for kinase reaction, and myelin basic protein (MBP) was used as control substrate for the kinase reaction. The kinase activity was monitored by autoradiography. Interestingly, kinase activity of STK31 resulting from double transfection with MAGEG2 was decreased by 29% compared with that of single transfection (**Figure 5c** and **5d**).

Table 1: Proteins associated with MAGEG2

Accession number	*Protein description*	*Matched peptide*	*Length (aa)*	*MW (Da)*	*pI*
IPI00133903.1ISWI	Hspa9 stress-70 protein, mitochondrial	16	679	73,528	6.2
IPI00118122.2ISWI	Stk31 serine/threonine-protein kinase 31	6	1018	115,018	5.4
IPI00454108.3ITRE	1700020D05Rik mage-g2 protein	5	294	33,443	9.2
IPI00135730.1ISWI	Arf2 ADP-ribosylation factor 2	4	181	20,746	6.6
IPI00224575.1ISWI	Hnrnpk heterogeneous nuclear ribonucleoprotein K isoform 2	3	464	51,028	5.3
IPI00271869.1ITRE	Gm3200 glyceraldehyde-3-phosphate dehydrogenase	2	333	36,031	8.4
IPI00136251.1ISWI	Dnaja2 DnaJ homolog subfamily A member 2	2	412	45,746	6.5
IPI00123494.3ISWI	Psmd2 26S proteasome non-ATPase regulatory subunit 2	2	908	100,203	5.2

aa: amino acid; MW: molecular weight; pI: isoelectric point

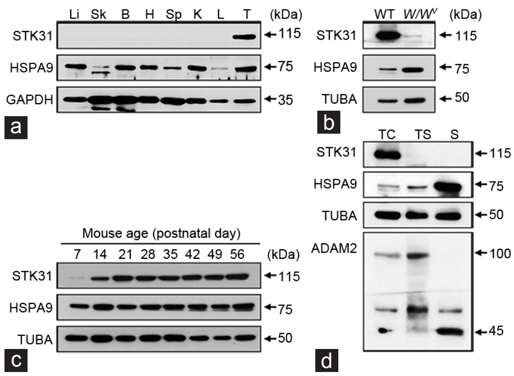

Figure 3: Expression profiles of putative binding partners, STK31 and HSPA9. The characterization of STK31 and HSPA9, western blot analysis was conducted using purchased antibodies against them. (**a**) Tissue distributions at the protein level were investigated with total cell lysates from different tissues of adult mice. Li: liver; Sk: skeletal muscle; B: brain; H: heart; Sp: spleen; K: kidney; L: lung; T: testis. Anti-GAPDH was used to estimate equivalent amounts of proteins in tissues. (**b**) Examination of testicular expression patterns by comparison between normal and germ cell-lacking testis. Total cell lysates were obtained from WT and *W/W^v* mutant mice. α-Tubulin was used as a loading control. (**c**) Determination of expression times in the testis of STK31 and HSPA9. Expression patterns were analyzed by immunoblotting of total cell lysates prepared from mouse testis at different days after birth (from 7 to 56 days). (**d**) Stage-specific expression patterns of STK31 and HSPA9. Protein samples from testicular germ cells (TC), testicular spermatozoa (TS), and mature spermatozoa (S) were immunoblotted with anti-STK31 and anti-HSPA9. ADAM2 and α-tubulin were included as reference proteins.

DISCUSSION

In the present study, we identified testis-specific Type II MAGE family member, mouse MAGEG2, at the transcriptional, protein, and functional levels for the first time. In general, type II MAGE family members are known to be expressed ubiquitously,[12,13] but MAGEG2 is different from other Type II MAGE members in that its expression is restricted to the testis. Although it was selected from Sertoli cell UniGene library at the beginning of our study, MAGEG2 was primarily expressed in the testicular germ cells and the expression level was increased obviously during pachytene stage. This indicates that the function of MAGEG2 is regulated in a stage-specific manner in the pachytene spermatocytes. *In vitro* analysis showed whole cell localization of MAGEG2, consistent with reported patterns of other mouse MAGEs.[12,13,18,19] Moreover, by means of a generated specific antibody, we carried out immunoprecipitation followed by MS analysis, in which we identified putative interaction partners. Among them, STK31 was considered as a strong partner with relatively high spectrum counts.

Stk31 was first reported as a male germ cell-specific gene[20,21] and it was also called as a Tudor-domain containing protein 8 (*Tdrd8*) on account of its conserved domain.[16,17] Consistent with previous reports, our western blot analysis using cognate antibodies presented germ cell-specific expression patterns. Moreover, through immunoblotting with germ cell-lacking testis (*W/W^v*), it is likely that STK31 is expressed not only in germ cells but also in somatic cells, with very low level in the testis. Besides, expression level at the early stages of development was similar to that of *W/W^v* mutant testis, indicating that STK31 shows less or no expression in the earlier stages of germ cell development. As the stage proceeds, the expression level increased significantly during the pachytene stage. These expression patterns were similar to those of MAGEG2, suggesting that STK31 has a close relationship with MAGEG2. In fact, we found that MAGEG2 suppresses the kinase activity of STK31 when associated with it in the testicular germ cells.

STK31 has been studied in male germ cells.[16,17,22] In particular, it has been reported that germ cell development is not affected in *Stk31* knockout mice,[17,22] suggesting the redundancy of STK31 with similar proteins. Recently, STK31 was characterized as a SUMO target of spermatocytes by means of co-immunoprecipitation analysis and immunofluorescent localization with SUMO-1,[23] suggesting a possible relationship between STK31 and sumoylation. In the testis, SUMO-1 starts to appear in early spermatocytes at low level, and its expression is increased during early- to mid-spermatocytes, corresponding to the pachytene stage.[5,24] From the distinct expression pattern, the functions of SUMO-1 in murine and human testes have been demonstrated to correlate with expression timing, such as meiotic sex chromosome inactivation (MSCI), XY body formation, and synaptonemal complex scaffold maintenance.[5,24–28] Although the expressions of SUMO-2 and -3 overlap, their functions seem to be different from those of SUMO1 and their roles in meiosis remain to be determined.[26,28] Regarding another suspected binding partner, HSPA9 has also been reported as a ubiquitous target of sumoylation through the MS analysis.[23,29,30] MAGE families have been reported as counterpart of SUMO E3 ligases.[31,32] Direct experimental evidence for relationship with sumoylation was not found in this study, although association with sumoylation in our research is predictable. It would seem that the antibody generated from the synthesized antigen peptide has a sensitivity limit. Alternatively, it is possible that there is no relationship between MAGEG2 and sumoylation.

In this study, direct interactions between MAGEG2 and the two proteins (HSPA9 and STK31) were detected, whereas direct interaction between HSPA9 and STK31 was not confirmed. Thus, we assume that they do not compose a functional single complex, and STK31 and HSPA9 bind to MAGEG2 separately. Molecular chaperones, the so-called heat shock proteins (HSPs), include various subfamilies with numerous members, and they are usually expressed in all tissues. This redundancy implies that they contain locally adapted secondary roles according to their expression organelles.[33]

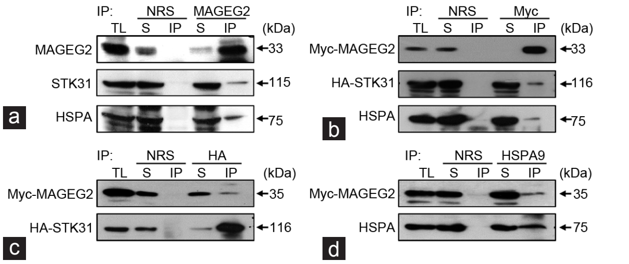

Figure 4: Association of MAGEG2 with putative bindings partners, STK31 and HSPA9. To confirm interactions with STK31 and HSPA9, immunoprecipitations (IP) were conducted *in vivo* and *in vitro*. (**a**) Interactions of endogenous MAGEG2 with STK31 and HSPA9 through co-IP with anti-MAGEG2. Co-immunoprecipitated STK31 and HSPA9 were detected by their cognate antibodies. Normal rabbit serum (NRS) was utilized as a negative control. (**b**) Examination of *in vitro* interactions using co-transfected HEK293T cell line with Myc-tagged MAGEG2 and HA-tagged STK31. HA-tagged STK31 and endogenous HSPA9 were pulled down by anti-Myc antibody for Myc-tagged MAGEG2. Normal mouse serum (NMS) was used as a negative control for anti-Myc. (**c**) Interaction between HA-tagged STK31 and Myc-tagged MAGEG2 *in vitro*. Myc-tagged MAGEG2 was detected from immunoprecipitated beads with anti-HA for HA-tagged STK31. IP with NRS was performed as a negative control. (**d**) Interaction between Myc-tagged MAGEG2 and endogenous HSPA9 *in vitro*. Transfected Myc-tagged MAGEG2 was pulled down by anti-HSPA9. NRS was used as a negative IgG for anti-HSPA9. TL: total cell lysate; S: supernatant; IP: immunoprecipitant.

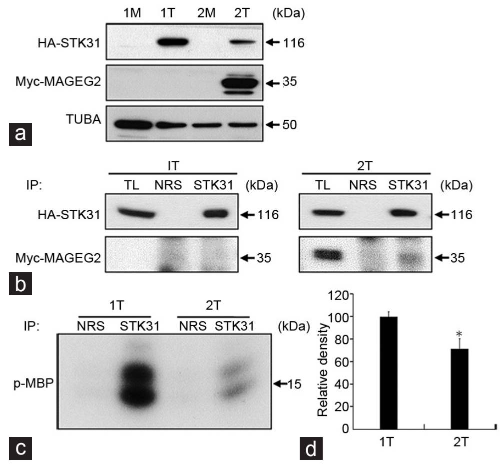

Figure 5: Functional study of MAGEG2 related with STK31. To identify functional role of MAGEG2, IP-kinase assay was carried. (**a**) Confirmation of single transfection with HA-tagged STK31 (1T) and double transfection using HA-tagged STK31 and Myc-tagged MAGEG2 (2T). α-Tubulin was used for normalization. (**b**) Examination of IP efficiency of anti-STK31. The immunoprecipitated complexes were immunoblotted to confirm existence of both HA-tagged STK31 and Myc-tagged MAGEG2 by cognate antibodies on the IP beads. Normal rabbit serum (NRS) was used as a negative control. (**c**) Autoradiography of immunoprecipitated beads by anti-STK31. Kinase activity of STK31 was estimated by autoradiography of myelin basic protein (MBP), labeled with ^{32}P. (**d**) Statistic comparison of kinase activity between single transfection and double transfection. The kinase activity was quantified by densitometry. Value represents the mean ± s.e.m. (n = 4); *P < 0.05 (Student's t-test). 1M: mock for single transfection using empty HA vectors; 1T: single transfection; 2M: mock for double transfection using empty HA vectors and Myc vectors; 2T: double transfection; IP: immunoprecipitation; TL: total cell lysate.

Viewed from this perspective, extensive investigations regarding secondary roles of HSPs in the testis have been reported related to spermatogenesis, and these findings have suggested new perspective for understanding spermatogenesis.[15,33–40] For example, among several HSP70 family members, the role of HSPA2 has been well characterized in spermatogenesis in knockout mice.[36] Functions related to spermatogenesis, such as regulation of G2/M phase transition,[37] chaperone activity for DNA packaging transition proteins,[35] role as a transitional protein for chromatin remodeling in spermatids,[15] and assembly of zona pellucida (ZP) binding complex for ZP binding,[39] have been reported. HSPA5 and HSPA8 were also identified in relation to male germ cell development. HSPA5 has been found to be expressed on the sperm surface, and several roles in different cell types of expression have been demonstrated.[34,38,40] In the case of HSPA8, it was revealed that the protein is associated with acrosome biogenesis in the rat testis[41] and the binding affinity to oviductal epithelium of the boar spermatozoa has been reported.[42]

On the basis of these previous studies, an interaction between HSPA9 and testis-specific MAGEG2 suggests a possibility for a secondary role of HSPA9 during prophase I of spermatogenesis. Preleptotene spermatocytes in the first wave of spermatogenesis suffer apoptotic cell death, resulting in large decrease of germ cells to maintain the germ cell population.[36,43] The regulatory role of HSPA9 in apoptosis has been reported,[44–46] but its function in male reproduction remains to be discovered. Perhaps, the MAGEG2/HSPA9 complex might have a regulatory function in apoptosis during early wave of spermatogenesis. It is also known that HSPA9 is involved in stress response. Various stressors upregulate HSPA9 to suppress the engagement of apoptosis and regulate the functions of the tumor suppressor protein p53.[47,48] Therefore, this raises another possibility that HSPA9 together with MAGEG2 could be related to stress response in the testis.

CONCLUSIONS

Our study provides insights for understanding the novel testis-specific protein, MAGEG2. Its expression is regulated stage specifically during spermatogenesis and the protein interacts with STK31 and HSPA9 separately. Regarding the interaction with STK31, the kinase activity of STK31 was reduced by association with MAGEG2, implying that MAGEG2 is involved in pachytene stage-specific protein phosphorylation mechanism. With regard to HSPA9, direct binding with HSPA9 suggests possibility of MAGEG2 as a chaperone component for male germ cell development. To clarify the functional mechanism of MAGEG2 and the binding proteins, further studies are necessary. To summarize, to our knowledge, this is the first study highlighting the characteristics of MAGEG2 in the mouse testis. This identification serves as a novel avenue for further studies on the regulatory roles of testis-specific MAGEs in male reproduction.

AUTHOR CONTRIBUTIONS

JJ and CC conceived and designed the experiments; JJ performed the experiments; JJ, ZYP, and CC analyzed the data; JJ, SJ, HC, JTK, Jihye K, Jaehwan K, and ZYP contributed reagents/materials/analysis tools; JJ and CC wrote the paper. All authors read and approved the final manuscript.

COMPETING INTERESTS

All authors declared no competing interests.

ACKNOWLEDGMENTS

This work was supported by the Mid-career Researcher Program through NRF grant funded by the MEST (NRF-2015R1A2A2A01005300), the Bio and Medical Technology Development Program of the National Research Foundation of Korea funded by the Ministry of Science, ICT and Future Planning (NRF-2013M3A9A7046297) and Systems Biology Infrastructure Establishment grant funded by GIST Research Institute (GRI) in 2016.

Supplementary information is linked to the online version of the paper on the *Asian Journal of Andrology* website.

REFERENCES

1 Griswold MD. The central role of Sertoli cells in spermatogenesis. *Semin Cell Dev Biol* 1998; 9: 411–6.
2 Hess RA, Renato de Franca L. Spermatogenesis and cycle of the seminiferous epithelium. *Adv Exp Med Biol* 2008; 636: 1–15.
3 Eddy EM. Male germ cell gene expression. *Recent Prog Horm Res* 2002; 57: 103–28.
4 Lee B, Jin S, Choi H, Kwon JT, Kim J, *et al*. Expression and Function of the testis-predominant protein LYAR in mice. *Mol Cells* 2013; 35: 54–60.
5 Vigodner M, Morris PL. Testicular expression of small ubiquitin-related modifier-1 (SUMO-1) supports multiple roles in spermatogenesis: silencing of sex chromosomes in spermatocytes, spermatid microtubule nucleation, and nuclear reshaping. *Dev Biol* 2005; 282: 480–92.
6 Simpson AJ, Caballero OL, Jungbluth A, Chen YT, Old LJ. Cancer/testis antigens, gametogenesis and cancer. *Nat Rev Cancer* 2005; 5: 615–25.
7 Chomez P, De Backer O, Bertrand M, De Plaen E, Boon T, *et al.* An overview of the MAGE gene family with the identification of all human members of the family. *Cancer Res* 2001; 61: 5544–51.
8 Doyle JM, Gao J, Wang J, Yang M, Potts PR. MAGE-RING protein complexes comprise a family of E3 ubiquitin ligases. *Mol Cell* 2010; 39: 963–74.
9 Scanlan MJ, Gure AO, Jungbluth AA, Old LJ, Chen YT. Cancer/testis antigens: an expanding family of targets for cancer immunotherapy. *Immunol Rev* 2002; 188: 22–32.
10 Sang M, Wang L, Ding C, Zhou X, Wang B, *et al*. Melanoma-associated antigen genes – an update. *Cancer Lett* 2011; 302: 85–90.
11 Guo L, Sang M, Liu Q, Fan X, Zhang X, *et al*. The expression and clinical significance of melanoma-associated antigen-A1, -A3 and -A11 in glioma. *Oncol Lett* 2013; 6: 55–62.
12 Barker PA, Salehi A. The MAGE proteins: emerging roles in cell cycle progression, apoptosis, and neurogenetic disease. *J Neurosci Res* 2002; 67: 705–12.
13 Xiao J, Chen HS. Biological functions of melanoma-associated antigens. *World J Gastroenterol* 2004; 10: 1849–53.
14 Phelps BM, Koppel DE, Primakoff P, Myles DG. Evidence that proteolysis of the surface is an initial step in the mechanism of formation of sperm cell surface domains. *J Cell Biol* 1990; 111: 1839–47.
15 Choi E, Han C, Park I, Lee B, Jin S, *et al*. A novel germ cell-specific protein, SHIP1, forms a complex with chromatin remodeling activity during spermatogenesis. *J Biol Chem* 2008; 283: 35283–94.
16 Bao J, Wang L, Lei J, Hu Y, Liu Y, *et al*. STK31(TDRD8) is dynamically regulated throughout mouse spermatogenesis and interacts with MIWI protein. *Histochem Cell Biol* 2011; 137: 377–89.
17 Zhou J, Leu NA, Eckardt S, McLaughlin KJ, Wang PJ. STK31/TDRD8, a Germ cell-specific factor, is dispensable for reproduction in mice. *PLoS One* 2014; 9: e89471.
18 Lavi-Itzkovitz A, Tcherpakov M, Levy Z, Itzkovitz S, Muscatelli F, *et al*. Functional consequences of necdin nucleocytoplasmic localization. *PLoS One* 2012; 7: e33786.
19 Devos J, Weselake SV, Wevrick R. Magel2, a Prader-Willi syndrome candidate gene, modulates the activities of circadian rhythm proteins in cultured cells. *J Circadian Rhythms* 2011; 9: 12.
20 Wang PJ, McCarrey JR, Yang F, Page DC. An abundance of X-linked genes expressed in spermatogonia. *Nat Genet* 2001; 27: 422–6.
21 Sabeur K, Ball BA, Corbin CJ, Conley A. Characterization of a novel, testis-specific equine serine/threonine kinase. *Mol Reprod Dev* 2008; 75: 867–73.
22 Bao J, Yuan S, Maestas A, Bhetwal BP, Schuster A, *et al.* Stk31 is dispensable for embryonic development and spermatogenesis in mice. *Mol Reprod Dev* 2013; 80: 786.
23 Xiao Y, Pollack D, Andrusier M, Levy A, Callaway M, *et al.* Identification of cell-specific targets of sumoylation during mouse spermatogenesis. *Reproduction* 2016; 151: 149–66.
24 Rogers RS, Inselman A, Handel MA, Matunis MJ. SUMO modified proteins localize to the XY body of pachytene spermatocytes. *Chromosoma* 2004; 113: 233–43.
25 Brown PW, Hwang K, Schlegel PN, Morris PL. Small ubiquitin-related modifier (SUMO)-1, SUMO-2/3 and SUMOylation are involved with centromeric heterochromatin of chromosomes 9 and 1 and proteins of the synaptonemal complex during meiosis in men. *Hum Reprod* 2008; 23: 2850–7.
26 Rodriguez A, Pangas SA. Regulation of germ cell function by SUMOylation. *Cell Tissue Res* 2015; 363: 47–55.
27 Vigodner M. Roles of small ubiquitin-related modifiers in male reproductive function. In: Kwang WJ, editor. International Review of Cell and Molecular Biology. Ch. 6. New York: Academic Press; 2011. p227–59.
28 La Salle S, Sun F, Zhang XD, Matunis MJ, Handel MA. Developmental control of sumoylation pathway proteins in mouse male germ cells. *Dev Biol* 2008; 321: 227–37.
29 Matafora V, D'Amato A, Mori S, Blasi F, Bachi A. Proteomics analysis of nucleolar SUMO-1 target proteins upon proteasome inhibition. *Mol Cell Proteomics* 2009; 8: 2243–55.
30 Vigodner M, Shrivastava V, Gutstein LE, Schneider J, Nieves E, *et al.* Localization and identification of sumoylated proteins in human sperm: excessive sumoylation is a marker of defective spermatozoa. *Hum Reprod* 2013; 28: 210–23.
31 Gur I, Fujiwara K, Hasegawa K, Yoshikawa K. Necdin Promotes ubiquitin-dependent degradation of PIAS1 SUMO E3 ligase. *PLoS One* 2014; 9: e99503.
32 Taylor EM, Copsey AC, Hudson JJ, Vidot S, Lehmann AR. Identification of the proteins, including MAGEG1, that make up the human SMC5-6 protein complex. *Mol Cell Biol* 2008; 28: 1197–206.
33 Dun MD, Aitken RJ, Nixon B. The role of molecular chaperones in spermatogenesis and the post-testicular maturation of mammalian spermatozoa. *Hum Reprod Update* 2012; 18: 420–35.
34 Mamelak D, Lingwood C. The ATPase domain of hsp70 possesses a unique binding specificity for 3'-sulfogalactolipids. *J Biol Chem* 2001; 276: 449–56.
35 Govin J, Caron C, Escoffier E, Ferro M, Kuhn L, *et al*. Post-meiotic shifts in HSPA2/HSP70.2 chaperone activity during mouse spermatogenesis. *J Biol Chem* 2006; 281: 37888–92.
36 Mori C, Nakamura N, Dix DJ, Fujioka M, Nakagawa S, *et al*. Morphological analysis of germ cell apoptosis during postnatal testis development in normal and Hsp70-2 knockout mice. *Dev Dyn* 1997; 208: 125–36.
37 Zhu D, Dix DJ, Eddy EM. HSP70-2 is required for CDC2 kinase activity in meiosis I of mouse spermatocytes. *Development* 1997; 124: 3007–14.
38 Han C, Park I, Lee B, Jin S, Choi H, *et al.* Identification of heat shock protein 5, calnexin and integral membrane protein 2B as Adam7-interacting membrane proteins in mouse sperm. *J Cell Physiol* 2011; 226: 1186–95.
39 Huszar G, Stone K, Dix D, Vigue L. Putative creatine kinase M-isoform in human sperm is identifiedas the 70-kilodalton heat shock protein HspA2. *Biol Reprod* 2000; 63: 925–32.
40 Naaby-Hansen S, Diekman A, Shetty J, Flickinger CJ, Westbrook A, *et al.* Identification of calcium-binding proteins associated with the human sperm plasma membrane. *Reprod Biol Endocrinol* 2010; 8: 6.
41 Yang C, Miao S, Zong S, Koide SS, Wang L. Identification and characterization of rDJL, a novel member of the DnaJ protein family, in rat testis. *FEBS Lett* 2005; 579: 5734–40.
42 Elliott RM, Lloyd RE, Fazeli A, Sostaric E, Georgiou AS, *et al.* Effects of HSPA8, an evolutionarily conserved oviductal protein, on boar and bull spermatozoa. *Reproduction* 2009; 137: 191–203.
43 Russell LD, Chiarini-Garcia H, Korsmeyer SJ, Knudson CM. Bax-dependent spermatogonia apoptosis is required for testicular development and spermatogenesis. *Biol Reprod* 2002; 66: 950–8.
44 Yoo JY, Ryu J, Gao R, Yaguchi T, Kaul SC, *et al.* Tumor suppression by apoptotic and anti-angiogenic effects of mortalin-targeting adeno-oncolytic virus. *J Gene Med* 2010; 12: 586–95.
45 Starenki D, Hong SK, Lloyd RV, Park JI. Mortalin (GRP75/HSPA9) upregulation promotes survival and proliferation of medullary thyroid carcinoma cells. *Oncogene* 2015; 34: 4624–34.
46 Chuanmei P, Pu Y, Yingbo C, Ming H, Leilei L, *et al*. HSPA9 overexpression inhibits apoptin-induced apoptosis in the HepG2 cell line. *Oncol Rep* 2013; 29: 2431–7.
47 Kaul SC, Deocaris CC, Wadhwa R. Three faces of mortalin: a housekeeper, guardian and killer. *Exp Gerontol* 2007; 42: 263–74.
48 Flachbartová Z, Kovacech B. Mortalin – A multipotent chaperone regulating cellular processes ranging from viral infection to neurodegeneration. *Acta Virol* 2013; 57: 3–15.
49 Zuckerkand E, Pauling L. Evolutionary divergence and convergence in proteins. In: Bryson V, Vogel HJ, editors. Evolving Genes and Proteins. New York: Academic Press; 1965. p97–166.

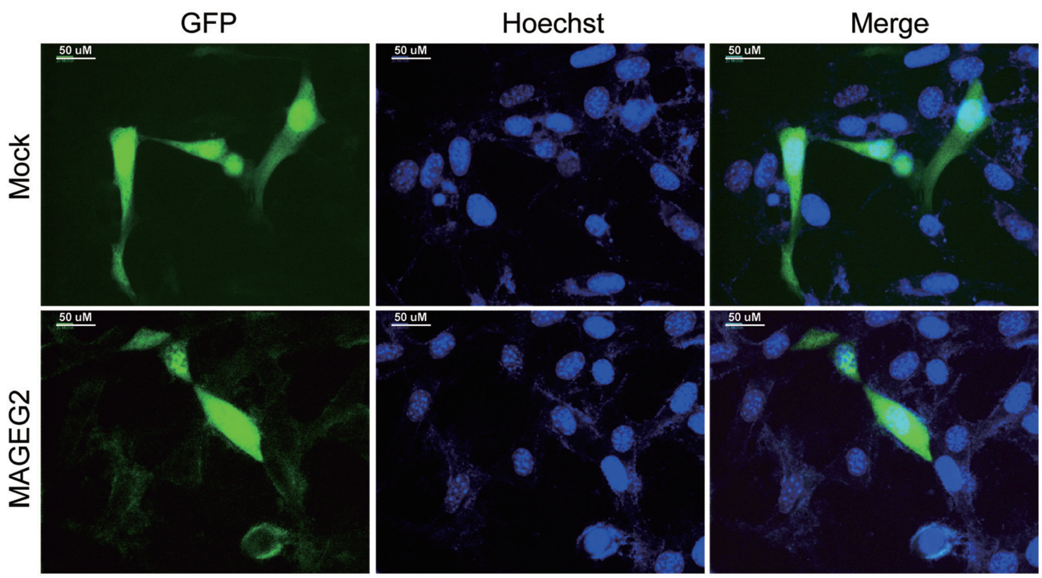

Supplementary Figure 1: Subcellular localization of MAGEG2. Subcellular localization of MAGEG2 in NIH3T3 cells. To examine the subcellular localization of protein encoded by Mageg2, NIH3T3 cells were transfected with full length of Mageg2-GFP construct. The empty pEGFP-N2 vector was utilized as a mock. The nucleus of the transfected cells were stained by Hoechst 33258. Scale bar = 50 µm.

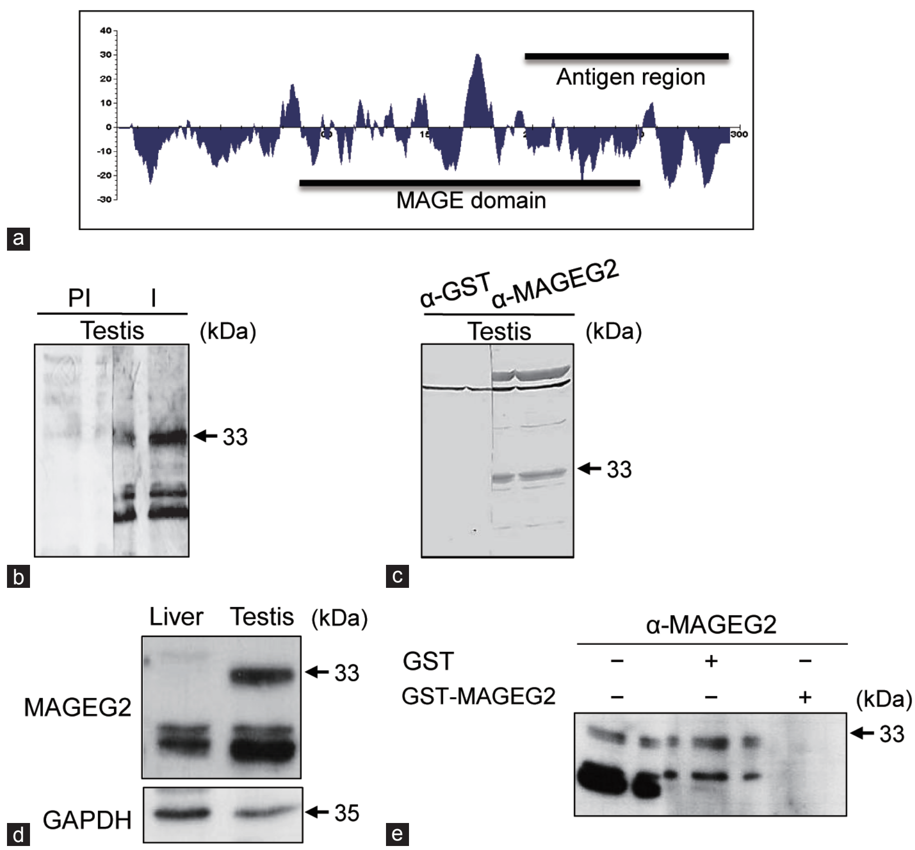

Supplementary Figure 2: Generation of antibodies against MAGEG2. To characterize of MAGEG2 at the protein level, we generated antibody against a mouse MAGEG2 recombinant fusion protein. (**a**) Antigen region for antibody generation. The diagram indicates hydrophobicity of MAGEG2. (**b**) Comparison between preboosted serum (PI) and postboosted serum (I) for activity test. The expected molecular weight was 33 kDa. (**c**) To verify specificity for MAGEG2, activity of anti-MAGEG2 antibody was compared to that of anti-glutathione S-transferase (GST) antibody purified from boosted serum. (**d**) Testis-specific band was examined by comparing expression patterns of total cell lysates between liver and testis. The antibody against GAPDH was used as a loading control. (**e**) GST or GST recombinant MAGEG2 (GST-MAGEG2) protein was added to the anti-MAGEG2 antibody buffer during incubation of Western blot analysis.

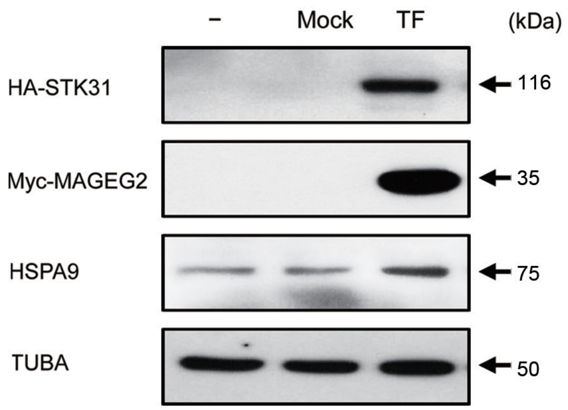

Supplementary Figure 3: Confirmation of transfection efficiency by Western blot analysis. Transfection of both HA-tagged STK31 and Myc-tagged MAGEG2 into HEK293T cell line was confirmed by Western blotting by cognate antibodies of them. The amount of endogenous HSPA9 was examined by Western blotting using anti-HSPA9. An anti-α-tubulin antibody was used as a control; –: not transfected cell lysates; TF: transfected cell lysates.

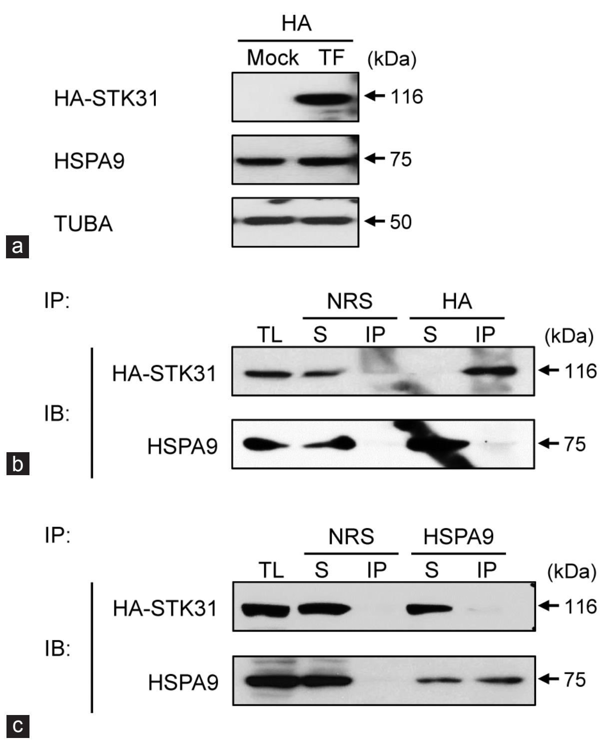

Supplementary Figure 4: Examination of binding between endogenous HSPA9 and transfected HA-tagged STK31 *in vitro* level. (**a**) HA-tagged STK31 was transfected into HEK293T cells. (**b**) Endogenous HSPA9 was not detected on the IP beads of HA-tagged STK31. Normal rabbit serum (NRS) was used as a negative control. (**c**) Direct binding between HSPA9 and HA-tagged STK31 was not found. NRS was utilized as a negative control. TF: transfected cell lysates; TL: total cell lysates; S, supernatant; IP: immunoprecipitant; IB: immunoblotting.